The Kinetics of Addition and Fragmentation in Reversible Addition Fragmentation Chain Transfer Polymerization: An ab Initio Study

Michelle L. Coote*

Research School of Chemistry, Australian National University, Canberra, ACT 0200, Australia

Received: August 26, 2004; In Final Form: November 20, 2004

High-level ab initio calculations of the forward and reverse rate coefficients have been performed for a series of prototypical reversible addition fragmentation chain transfer (RAFT) reactions: R• + S═C(Z)SCH_3 → R−SC•(Z)SCH_3, for R = CH_3, with Z = CH_3, Ph, and CH_2Ph; and Z = CH_3, with R = (CH_3), CH_2COOCH_3, CH_2Ph, and $C(CH_3)_2CN$. The addition reactions are fast (ca. 10^6−10^8 L mol^{-1} s^{-1}), typically around three orders of magnitude faster than addition to the C═C bonds of alkenes. The fragmentation rate coefficients are much more sensitive to the nature of the substituents and vary from 10^{-4} to 10^7 s^{-1}. In both directions, the qualitative effects of substituents on the rate coefficients largely follow those on the equilibrium constants of the reactions, with fragmentation being favored by bulky and radical-stabilizing R-groups and addition being favored by bulky and radical-stabilizing Z-groups. However, there is evidence for additional polar and hydrogen-bonding interactions in the transition structures of some of the reactions. Ab initio calculations were performed at the G3(MP2)-RAD//B3-LYP/6-31G(d) level of theory, and rates were obtained via variational transition state theory in conjunction with a hindered-rotor treatment of the low-frequency torsional modes. Various simplifications to this methodology were investigated with a view to identifying reliable procedures for the study of larger polymer-related systems. It appears that reasonable results may be achievable using standard transition state theory, in conjunction with ab initio calculations at the RMP2/6-311+G(3df,2p) level, provided the results for delocalized systems are corrected to the G3(MP2)-RAD level using an ONIOM-based procedure. The harmonic oscillator (HO) model may be suitable for qualitative "order-of-magnitude" studies of the kinetics of the individual reactions, but the hindered-rotor (HR) model is advisable for quantitative studies.

1. Introduction

In recent years, the field of free-radical polymerization has been revolutionalized by the development of controlled/living radical polymerization processes, including nitroxide-mediated polymerization (NMP),[1] atom transfer polymerization (ATRP),[2] and reversible addition fragmentation chain transfer (RAFT) polymerization.[3] By protecting the majority of the growing polymer chains from the bimolecular termination reactions that normally occur in free-radical polymerization, such processes facilitate the production of polymers with narrow molecular weight distributions, well-defined end groups, and complex architectures such as star polymers and block copolymers. Such polymers can be used in a range of technological applications, including light-emitting nanoporous films,[4] nanostructured carbon arrays,[5] light-harvesting polymers,[6] and pH-induced self-assembling polymeric micelles.[7,8]

The basic principle of controlled radical polymerization is to protect the majority of growing polymer chains (at any point in time) from bimolecular termination, through their reversible trapping into a dormant form. In the RAFT process, which was developed by the CSIRO group[3] and utilizes the small-radical chemistry of Zard and co-workers,[9] thiocarbonyl compounds (known as RAFT agents, **2**) reversibly react with the growing polymeric radical (**1**) via the chain transfer reaction shown in Scheme 1, producing a polymeric thiocarbonyl compound (**4**) as the dormant species.[3]

SCHEME 1

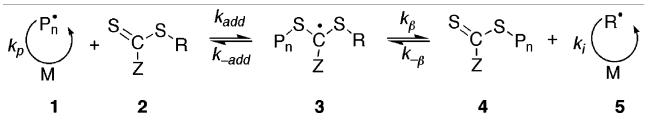

1 **2** **3** **4** **5**

To achieve control, a delicate balance of the forward and reverse rates of addition (k_{add} and k_{-add}) and fragmentation (k_β and $k_{-\beta}$), together with the rates of reinitiation (k_i) and propagation (k_p), is required, so as to ensure that the dormant species is orders-of-magnitude greater in concentration than the active species and that the exchange between the two forms is rapid. It is therefore important to understand the effects of substituents on each of these individual steps, so that RAFT agents (and other reaction conditions) can be optimized for the controlled polymerization of any given monomer.

To study the effect of substituents on the RAFT process, accurate measurements of the rate coefficients for the individual steps are important. Unfortunately, owing to the complexity of the reaction kinetics, these are difficult to access from conventional kinetic measurements. Instead, they must be inferred from related observable quantities such as the overall rate of polymerization, the overall radical concentration, and the molecular weight distribution of the resulting polymer. In doing so, it is necessary to make kinetic-model-based assumptions, and such assumptions have recently been a source of controversy with regard to certain RAFT polymerization systems. In particular, depending upon the assumptions made, alternative measure-

* E-mail address for correspondence. E-mail: mcoote@rsc.anu.edu.au.

10.1021/jp046131u CCC: $30.25
Published on Web 01/15/2005

ments of the fragmentation rate coefficient (k_β) for the cumyl dithiobenzoate (CDB)-mediated polymerization of styrene at 60 °C differ by six orders of magnitude.[10−14] Not only do such discrepancies make it difficult to study the effects of substituents in these reactions, but the alternative estimates of the fragmentation rate in RAFT polymerization (and the kinetic assumptions upon which they are based) also have completely different mechanistic implications for the RAFT process itself. More specifically, the lower values imply that the RAFT-adduct radical (**3**) is a long-lived species capable of functioning as a radical sink in its own right, and the higher values imply that the RAFT-adduct radical is a short-lived species, consumed in bimolecular termination reactions.

Ab initio molecular orbital calculations, which allow for the calculation of the rate and equilibrium constants for these reactions directly (i.e., without recourse to kinetic-model-based assumptions), can provide a means of resolving this discrepancy and discriminating between the alternative kinetic mechanisms.[15] Recently, ab initio calculations of the equilibrium constants ($K = k_{add}/k_\beta$) for model RAFT systems were used to support the lower values of the fragmentation rate coefficients and, hence, the notion that the RAFT-adduct radical is a relatively long-lived species.[16−18] It was possible in these previous studies to focus on the *thermodynamics* of the addition−fragmentation equilibrium because, unlike the fragmentation step, the experimental estimates of the rates of addition (ca. 10^5−10^6 L mol^{-1} s^{-1} at 60 °C for the styrene/CDB system)[10,13,19] are in general consensus with one another. Nonetheless, as this controversy highlights, the a priori calculation of reaction rates for these systems would provide a useful complement to experiment, given the problems with measuring such parameters experimentally. Such calculations could assist in the study of substituent effects, help to resolve other mechanistic issues (as recently demonstrated for the case of xanthate-mediated polymerization of vinyl acetate[20]), and ultimately provide a relatively inexpensive method for designing and testing novel RAFT agents.

In the present work, as a first step toward understanding the kinetics of the addition and fragmentation reactions in the RAFT process, the forward and reverse rate coefficients are calculated for six prototypical reactions:

$$\bullet CH_3 + S{=}C(CH_3)SCH_3 \rightarrow CH_3{-}SC\bullet(CH_3)SCH_3 \quad (1)$$

$$\bullet CH_3 + S{=}C(Ph)SCH_3 \rightarrow CH_3{-}SC\bullet(Ph)SCH_3 \quad (2)$$

$$\bullet CH_3 + S{=}C(CH_2Ph)SCH_3 \rightarrow CH_3{-}SC\bullet(CH_2Ph)SCH_3 \quad (3)$$

$$\bullet CH_2COOCH_3 + S{=}C(CH_3)SCH_3 \rightarrow CH_2(COOCH_3){-}SC\bullet(CH_3)SCH_3 \quad (4)$$

$$\bullet CH_2Ph + S{=}C(CH_3)SCH_3 \rightarrow CH_2(Ph){-}SC\bullet(CH_3)SCH_3 \quad (5)$$

$$\bullet C(CH_3)_2CN + S{=}C(CH_3)SCH_3 \rightarrow C(CH_3)_2(CN){-}SC\bullet(CH_3)SCH_3 \quad (6)$$

In reactions 1−3, the effects of the so-called Z-substituent (in the RAFT agent S=C(Z)SR) are examined, while reactions 4−6 are used to study the effects of the R-group. The substituents chosen for this study include small radical models of the propagating species in styrene (i.e., $\bullet CH_2Ph$) and methyl acrylate (i.e., $\bullet CH_2COOCH_3$) polymerization and some of the R- and Z-substituents found in typical RAFT agents. By focusing on small model reactions, it is possible to calculate the rate coefficients at a high level of theory, and in the present work, G3(MP2)-RAD//B3-LYP/6-31G(d) ab initio calculations are combined with variational transition-state theory and a one-dimensional hindered-rotor treatment of the low-frequency torsional modes. However, such calculations are currently not practicable for some of the larger-polymer related systems, and hence, as part of the present study, the effects of various simplifications to this methodology on the accuracy of the results are examined.

2. Computational Procedures

Forward and reverse rate coefficients were calculated for the addition of carbon-centered radicals (R•) to the sulfur center of the dithioester compounds (or "RAFT agents"), S=C(Z)SCH$_3$ for R = CH$_3$, with Z = CH$_3$, Ph, and CH$_2$Ph; and Z = CH$_3$, with R = (CH$_3$), CH$_2$COOCH$_3$, CH$_2$Ph, and C(CH$_3$)$_2$CN. Rate coefficients were obtained via variational transition-state theory in conjunction with a full (one-dimensional) hindered-rotor treatment of the low-frequency torsional modes, using ab initio calculations at the G3(MP2)-RAD//B3-LYP/6-31G(d) level. These calculations will now be described in more detail.

Standard ab initio molecular orbital theory[21] and density functional theory (DFT)[22] calculations were carried out using *Gaussian 98*[23] and *MOLPRO 2000.6*.[24] Unless noted otherwise, calculations on radicals were performed with an unrestricted wavefunction. In cases where a restricted open-shell wavefunction has been used, it is designated with an "R" prefix. The geometries of the reactants, products, and transition structures were optimized at the B3-LYP/6-31G(d) level of theory. For each species considered, care was taken to ensure that the optimized structure was the global (rather than merely local) minimum-energy structure by first performing extensive conformational searches at the HF/6-31G(d) level. Using the B3-LYP/6-31G(d)-optimized structures, we could then obtain improved energies at the RMP2/6-311+G(3df,2p) and G3(MP2)-RAD[25] levels of theory. The G3(MP2)-RAD barriers were used to evaluate the rate coefficients for the reactions, while the lower-cost RMP2/6-311+G(3df,2p) barriers were used to locate the variational transition structure (see following text). A previous assessment study for radical addition to C=S double bonds[26] indicated that the geometries and frequencies for these reactions are well-described at the B3-LYP/6-31G(d) level of theory, provided an IRCmax procedure[27] is used to correct the transition structure geometries. In the present work, this IRCmax procedure is effectively applied through the use of RMP2/6-311+G(3df,2p) energies in the variational transition-state theory calculations (see following text). The same assessment study indicated that high-level composite methods, such as G3(MP2)-RAD, are required for the calculation of accurate absolute values for the barriers and enthalpies of these reactions, while the lower-cost RMP2/6-311+G(3df,2p) procedure could provide reasonable absolute values (typically within 10 kJ mol^{-1}) and excellent relative values (within 4 kJ mol^{-1}). The accuracy of the RMP2/6-311+G(3df,2p) level of theory for the more specific case of RAFT polymerization will be examined as part of the present study.

Rate coefficients $k(T)$'s were calculated at 333.15 K via canonical variational transition-state theory, using the standard formulas:[28,29]

$$k(T) = \kappa(T)\frac{k_B T}{h}(c^\circ)^{1-m} e^{(-\Delta G^\ddagger/RT)} = \kappa(T)\frac{k_B T}{h}(c^\circ)^{1-m}\frac{Q_\ddagger}{\prod_{\text{reactants}} Q_i} e^{(-\Delta E^\ddagger/RT)} \quad (7)$$

where $\kappa(T)$ is the tunneling correction factor, T is the temperature (333.15 K), k_B is Boltzmann's constant ($1.380\,658 \times 10^{-23}$ J mol^{-1} K^{-1}), h is Planck's constant ($6.626\,075\,5 \times 10^{-34}$ J s), c° is the standard unit of concentration (mol L^{-1}), R is the universal gas constant (8.3142 J mol^{-1} K^{-1}), $Q_\ddagger$ and Q_i are the molecular partition functions of the transition structure and reactant i, respectively, $\Delta G^\ddagger$ is the Gibb's free energy of activation, and $\Delta E^\ddagger$ is the 0 K, zero-point energy corrected energy barrier for the reaction. The value of c° depends on the standard-state concentration assumed in calculating the thermodynamic quantities (and translational partition function). In the present work, these quantities were calculated for 1 mol of an ideal gas at 333.15 K and 1 atm, and hence, $c^\circ = 0.036\,597\,1$ mol L^{-1}.

The tunneling coefficient $\kappa(T)$ corrects for quantum effects in motion along the reaction path.[30−33] While tunneling is important in certain chemical reactions (such as hydrogen abstraction), it can be assumed to be negligible (i.e., $\kappa \approx 1$) for the addition of carbon-centered radicals to thiocarbonyl compounds at the temperature of the present study (333.15 K). This is because the masses of the rearranging atoms are large and the barriers for the reactions are relatively broad, a feature evident in the low imaginary frequencies for the six reactions (which fall into the range $257i-339i$ cm^{-1}). In the present work, the validity of this assumption was confirmed by calculating approximate Eckart tunneling coefficients[34] using the imaginary frequency as an estimate of the curvature of the potential energy surface, as described previously.[35] This simplified one-dimensional procedure was only applicable to the four reactions in which the forward and reverse barriers were both positive, but in these four cases, the tunneling coefficient was less than 1.1 at 333.15 K.

The partition functions and associated thermodynamic quantities (H and S) were evaluated from the calculated geometries, frequencies, and energies, using standard formulas based on the statistical thermodynamics of an ideal gas, under the rigid-rotor/harmonic oscillator approximation.[28,29] However, in evaluating the vibrational partition functions, the accuracy was improved by treating all low-frequency (<300 cm^{-1}) torsional modes as one-dimensional hindered internal rotations. For each mode, rotational potentials were evaluated at the B3-LYP/6-31G(d) level of theory by scanning through 360° in steps of 10°. In keeping with previous recommendations,[36] relaxed (rather than frozen) scans were used. The contribution of these modes to the total entropy and enthalpy were then calculated via standard methods, as follows. For those modes having rotational potentials that could be described by a simple cosine function, the tables of Pitzer and co-workers were used.[37,38] In using the Pitzer tables, the reduced moment of inertia (I_r) was calculated using the equation for I,[2,3] as defined by East et al.[39] For the more complex modes, the rotational potentials $V(\theta)$'s were fitted with a Fourier series of up to 18 terms, and the corresponding energy levels were found by numerically solving the one-dimensional Schrödinger equation (eq 8) for a rigid rotor, using a Fortran program described previously.[40−42] The reduced moment of inertia (I_r) was again calculated using the equation for I,[2,3] as defined by East et al.[39] The resulting energy levels ϵ_i's were

$$-\frac{h^2}{8\pi I_r}\frac{\partial^2\Psi}{\partial\theta^2} + V(\theta)\Psi = \epsilon\Psi \quad (8)$$

then summed to obtain the partition function at the specified temperature, as follows:

$$Q_{\text{int rot}} = \frac{1}{\sigma_{\text{int}}}\sum_i \exp\left(-\frac{\epsilon_i}{k_B T}\right) \quad (9)$$

where σ_{int} is the symmetry number associated with that rotation. This latter approach yields identical values to those of the Pitzer tables for the special case of simple cosine potentials. It should be noted that, in this method, the low-frequency torsional modes have been approximated as one-dimensional rigid rotors, while in practice, these modes can be coupled with one another. However, a recent study of coupled internal rotations in another radical addition reaction (ethyl benzyl radical addition to ethene) indicated that the errors incurred in using a one-dimensional treatment are relatively minor, particularly when compared with the errors incurred under the harmonic oscillator approximation.[43]

In the present work, variational rather than standard transition-state theory was used. While there are a number variants of this theory,[33] the general approach is to evaluate the rate coefficient using as the transition structure the geometry corresponding to the maximum value of $\Delta G^\ddagger$ along the minimum energy path (MEP) of the reaction. In contrast, in standard transition-state theory, the transition-state geometry is located at the maximum value of $\Delta E^\ddagger$ along the MEP and is thus a first-order saddle point in the potential energy surface. Variational transition-state theory is more computationally expensive than standard transition-state theory but generally yields more accurate values for the reaction rates, particularly when (as in the present work) the reaction barriers are low or nonexistent.

Owing to the large size of the systems, a composite approach to calculating the variational rate coefficients was adopted in the present work. The values of $\Delta G^\ddagger$ along the MEP of the reaction were first calculated with a low-cost procedure in which energies were obtained at the RMP2/6-311+G(3df,2p)//B3-LYP/6-31G(d) level and entropies were calculated using B3-LYP/6-31G(d) geometries and frequencies in conjunction with the harmonic oscillator approximation. Having identified the variational transition structure, the energy calculations were then improved to the G3(MP2)-RAD level, and all low-frequency torsional modes (in the reactants, products, and transition structures) were treated as one-dimensional hindered internal rotations. It should be noted that because the values of $\Delta H^\ddagger$ along the reaction path were calculated at the RMP2/6-311+G(3df,2p)//B3-LYP/6-31G(d) level of theory, rather than the B3-LYP/6-31G(d) level, the use of variational transition-state theory actually served two purposes. Not only was the location of the transition structure corrected for entropic effects, but the reaction coordinate was also effectively optimized at the higher RMP2/6-311+G(3df,2p) level, as in the IRCmax procedure.[27] The determination of the variational transition structures is now described in more detail.

The formal transition structures of the reactions were first optimized (as first-order saddle points) at the B3-LYP/6-31G(d) level of theory. The MEP for the reaction was then calculated via an "IRC" calculation in *Gaussian* (which implements the algorithm of Gonzalez and Schlegel[44,45]), using a step size of 0.01 bohr amu$^{0.5}$ and the "verytight" convergence criteria. At each geometry along this MEP, the frequencies were calculated at the B3-LYP/6-31G(d) level of theory, and improved energies

TABLE 1: Forward (L mol^{-1} s^{-1}) and Reverse (s^{-1}) Rate Coefficients, and Associated Thermodynamic Functions, for R• + S=C(Z)SCH$_3$ → R−SC•(Z)SCH$_3$ at 60°C[a]

TS[b]	Z	R	$\Delta E^{\ddagger}$	$\Delta H^{\ddagger}$	$\Delta S^{\ddagger}$	$\Delta G^{\ddagger}$	k
			Forward Direction (Addition)				
1	CH_3	CH_3	13.0	9.2	−129.5	52.3	1.18×10^6
2	phenyl	CH_3	4.8	0.6	−123.5	41.7	5.47×10^7
3	benzyl	CH_3	8.4	4.4	−127.3	46.8	8.79×10^6
4	CH_3	CH_2COOCH_3	−14.5	−12.8	−157.1	39.6	1.19×10^8
5	CH_3	benzyl	3.7	4.9	−135.3	50.0	2.76×10^6
6	CH_3	$C(CH_3)_2CN$	−3.1	−0.9	−162.6	53.3	8.29×10^5
			Reverse Direction (Fragmentation)				
1	CH_3	CH_3	77.2	76.8	−10.8	80.4	1.73
2	phenyl	CH_3	100.1	99.3	−13.4	103.8	3.67×10^{-4}
3	benzyl	CH_3	80.7	79.3	−28.0	88.7	8.63×10^{-2}
4	CH_3	CH_2COOCH_3	43.6	39.7	−29.0	49.4	1.27×10^5
5	CH_3	benzyl	37.9	35.6	−26.8	44.6	7.15×10^5
6	CH_3	$C(CH_3)_2CN$	30.9	29.7	−7.6	32.2	6.21×10^7

[a] Calculated using variational transition state theory in conjunction with the hindered-rotor model at the G3(MP2)-RAD//B3-LYP/6-31G(d) level of theory. The barriers ($\Delta E^{\ddagger}$, kJ mol^{-1}), enthalpies of activation ($\Delta H^{\ddagger}$, kJ mol^{-1}), entropies of activation ($\Delta S^{\ddagger}$, J mol^{-1} K^{-1}) and Gibb's free energy of activation ($\Delta G^{\ddagger}$, kJ mol^{-1}) were evaluated using the variationally determined transition state, obtained as the maximum in $\Delta G^{\ddagger}$ (at 60 °C) along the minimum energy path. [b] See Figure 1.

were calculated at the RMP2/6-311+G(3df,2p) level. In the present work, a projection algorithm was not used for the calculation of the frequencies at geometries along the reaction path, because only relatively small displacements from the formal transition structures were considered. In preliminary studies (in which corresponding projected[46] and nonprojected frequencies were compared for geometries along the MEP of the related reaction, •CH$_3$ + S=C(H)SCH$_3$), it was found that, close to the transition structure, the error incurred in using standard (rather than projected) frequencies was smaller than the numerical noise in the projection algorithm[46] (as implemented in *Gaussian 98*). Having obtained the RMP2/6-311+G(3df,2p) energies and the B3-LYP/6-31G(d) geometries and frequencies, partition functions and associated thermodynamic quantities (H and S) were evaluated using the standard formulas based on the statistical thermodynamics of an ideal gas, under the rigid-rotor/harmonic oscillator approximation.[28,29] These were then used to calculate the corresponding values of $\Delta H^{\ddagger}$, $\Delta S^{\ddagger}$, and $\Delta G^{\ddagger}$ along the reaction path, and the variational transition structure was located as the geometry corresponding to the maximum value of $\Delta G^{\ddagger}$. Having located the variational transition structure, we could then obtain more accurate values of $\Delta H^{\ddagger}$, $\Delta S^{\ddagger}$, and $\Delta G^{\ddagger}$ using the higher G3(MP2)-RAD//B3-LYP/6-31G(d) level of theory, in conjunction with the more accurate hindered-rotor treatment of the low-frequency torsional modes, as described already.

3. Results and Discussion

Forward and reverse rate coefficients were calculated for the prototypical RAFT reactions 1−6 at 60 °C (see Table 1). The transition structures for the six reactions are displayed in Figure 1, while full geometries in the form of Gaussian archive entries are provided in the Supporting Information (Table S1). Also included in the Supporting Information are the full rotational potentials (or barriers for the modes with simple cosine potentials) used in calculating the partition functions for the low-frequency torsional modes (Tables S2 and S3) and also the values of $\Delta H^{\ddagger}$, $-T\Delta S^{\ddagger}$, and $\Delta G^{\ddagger}$ along the MEP, as used in locating the variational transition structures (Table S4). For reaction 1, these latter data are plotted as a function of the forming S···C bond length (Å) in Figure 2; corresponding graphs for all six reactions are provided in Figure S4 of the Supporting Information. In what follows, some methodological aspects of the calculation of the rate coefficients are examined, followed by a brief discussion of the effects of substituents on the reactions. The effects of substituents on the equilibrium constants of these reactions are discussed elsewhere.[17]

Methodological Aspects. In the present work, rate coefficients have been calculated at a high level of theory, G3(MP2)-RAD//B3-LYP/6-31G(d), using variational transition-state theory in conjunction with a full hindered-rotor treatment of the low-

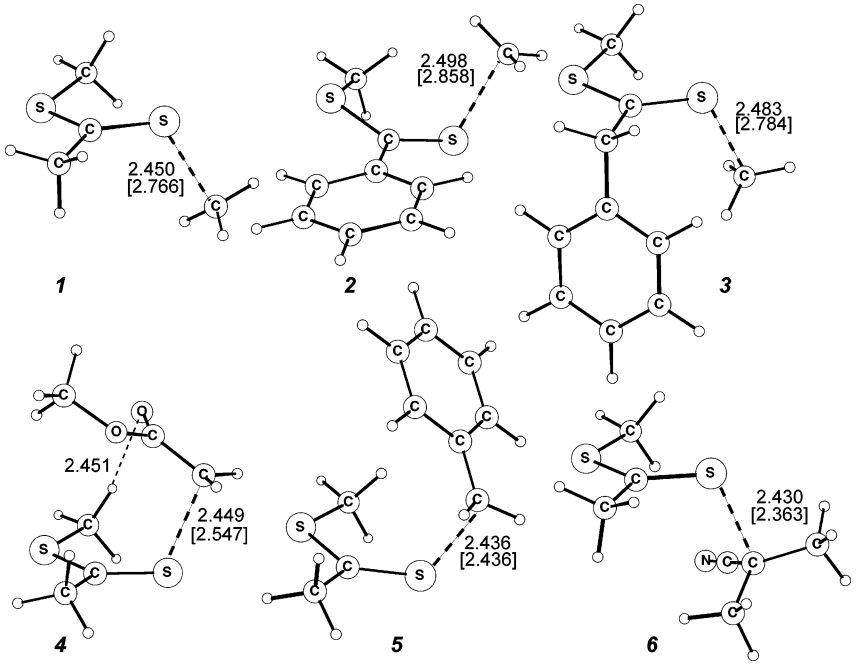

Figure 1. B3-LYP/6-31G(d) optimized geometries for the (variationally determined) transition structures for prototypical RAFT reactions 1−6. For each transition structure, the top number refers to the forming S···C bond length (Å) at the variational transition structure, while the number in square brackets is the corresponding value in the formal transition structure. The additional H-bonding distance in **4** refers to the variational transition structure.

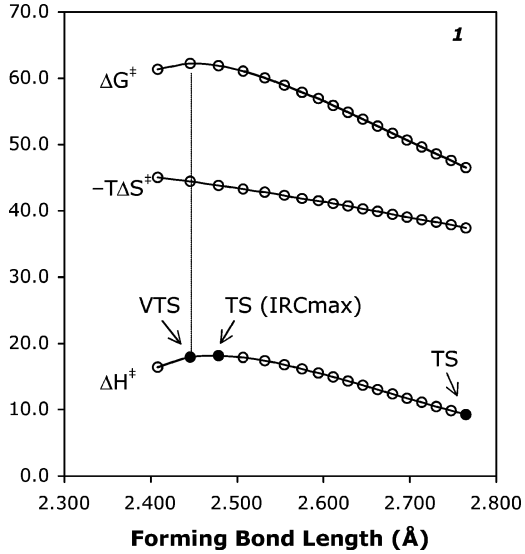

Figure 2. Values of $\Delta G^{\ddagger}$, $-T\Delta S^{\ddagger}$, and $\Delta H^{\ddagger}$ (kJ mol^{-1}) along the minimum energy path for the reaction, $\bullet CH_3 + S{=}C(CH_3)SCH_3 \rightarrow CH_3SC\bullet(CH_3)SCH_3$. The locations of the formal transition structure at B3-LYP/6-31G(d) (TS), the IRCmax transition structure at RMP2/6-311+G(3df,2p)//B3-LYP/6-31G(d) (IRCmax), and the variationally optimized transition structure at the RMP2/6-311+G(3df,2p)//B3-LYP/6-31G(d) level (VTS) are shown. Note that, for the sake of clarity, the energies are plotted as functions of the forming bond lengths. However, they correspond to points on the minimum energy path of the reaction, which was calculated as a function of the intrinsic reaction coordinate (in mass weighted units).

frequency torsional modes. This computationally intensive approach is not currently practicable for many of the larger, polymer-related systems, and it is therefore of interest to explore the effect of simplifications to this methodology on the accuracy of the calculated results. The accuracy of the ab initio calculations for studying radical addition to C═S bonds has already been extensively assessed in prototypical systems, such as $\bullet CH_3 + S{=}C(CH_3)_2$, from which it was concluded that the RMP2/6-311+G(3df,2p) level of theory should provide a suitable lower-cost method for such reactions.[26] In contrast, hybrid DFT methods, such as B3-LYP and MPW1K,[47] performed poorly for the barriers and enthalpies of these reactions.[26] In a more recent study, it was confirmed that the RMP2/6-311+G(3df,-2p) level of theory generally provides good results for the *thermodynamics* of model RAFT reactions of the form R• + S═C(Z)SR′, except when R• is a highly delocalized radical, such as benzyl.[48] In what follows, the performance of the RMP2/6-311+G(3df,2p) method for the calculation of reaction *barriers* in the model RAFT reactions is examined, together with other aspects of the kinetics calculations, such as the accuracy of the harmonic oscillator approximation.

Table 2 shows the forward and reverse barrier heights for the six reactions, calculated at both the G3(MP2)-RAD and RMP2/6-311+G(3df,2p) levels of theory and evaluated at the variational transition structure, the formal B3-LYP/6-31G(d) optimized transition structure and also the RMP2/6-311+G-(3df,2p)//B3-LYP/6-31G(d) IRCmax[27,49] transition structure. The IRCmax transition structure corresponds to the geometry that yields the maximum value of $\Delta E^{\ddagger}$ (rather than $\Delta G^{\ddagger}$) along the RMP2/6-311+G(3df,2p)//B3-LYP/6-31G(d) MEP of the reaction (see Figure 2). It differs from the formal B3-LYP/6-31G-(d) optimized transition structure (which also corresponds to the maximum value of $\Delta E^{\ddagger}$ along the MEP) in that the IRCmax transition structure is located using the higher-level RMP2/6-311+G(3df,2p)//B3-LYP/6-31G(d) MEP, rather than the B3-LYP/6-31G(d) MEP. In this way, the reaction coordinate (often the most sensitive part of a geometry optimization) is effectively optimized at the higher level of theory. Although previous studies have questioned the accuracy of this dual-level approach for the calculation of the rates of hydrogen abstraction reactions,[50] the IRCmax method has previously[26] been shown to improve the B3-LYP/6-31G(d)-optimized transition structures for radical addition to C═S bonds and should thus be suitable for the RAFT reactions of the present work.

TABLE 2: Effect of Level of Theory on the Barrier Heights (0 K, kJ mol^{-1}) for R• + S═C(Z)SCH$_3$ → R−SC•(Z)SCH$_3$ at 60 °C[a]

			G3(MP2)-RAD		RMP2/6-311+G(3df,2p)		
TS[b]	Z	R	VTS	TS	VTS	IRCmax TS	TS
Forward Direction (Addition)							
1	CH_3	CH_3	13.0	10.6	21.3	21.4	10.8
2	phenyl	CH_3	4.8	5.5	14.2	14.8	4.9
3	benzyl	CH_3	8.4	5.7	14.5	14.5	5.2
4	CH_3	CH_2COOCH_3	−14.5	−14.4	−14.9	−14.9	−16.1
5	CH_3	benzyl	3.7	3.7	−8.7	−8.3	−8.7
6	CH_3	$C(CH_3)_2CN$	−3.1	−4.6	−9.3	−9.3	−12.3
Reverse Direction (Fragmentation)							
1	CH_3	CH_3	77.2	74.8	83.5	83.6	73.1
2	phenyl	CH_3	100.1	100.7	105.3	105.9	96.0
3	benzyl	CH_3	80.7	78.0	83.9	83.9	74.6
4	CH_3	CH_2COOCH_3	43.6	43.7	44.1	44.2	42.9
5	CH_3	benzyl	37.9	37.9	38.8	39.2	38.8
6	CH_3	$C(CH_3)_2CN$	30.9	29.3	30.8	30.8	27.8

[a] Barrier heights were calculated at the G3(MP2)-RAD or RMP2/6-311+G(3df,2p) levels of theory using B3-LYP/6-31G(d) optimized geometries and include scaled B3-LYP/6-31G(d) zero-point vibrational energy corrections. The VTS values were evaluated using the variationally optimized transition structure geometries, the TS values were evaluated using the formal B3-LYP/6-31G(d) optimized transition structures, and the IRCmax values were evaluated at the maximum value of $\Delta E^{\ddagger}$ along the RMP2/6-311+G(3df,2p)//B3-LYP/6-31G(d) minimum-energy path. [b] See Figure 1.

Examining Table 2, we first note that that at the G3(MP2)-RAD level of theory the barriers at the formal and variational transition structures do not differ substantially. The maximum errors, which occur for the $\bullet CH_3$ addition reactions, are less than 3 kJ mol^{-1}, despite the fact that the variational transition structures have substantially shorter (by 0.3−0.4 Å) forming bonds than the formal transition structures. At the RMP2/6-311+G(3df,2p) level of theory, the corresponding difference in barrier heights is substantially larger for these reactions (up to 10.5 kJ mol^{-1}), but the additional error is almost entirely corrected via the IRCmax technique (the differences between the IRCmax and variational transition structures being less than 1 kJ mol^{-1} in all cases). It thus seems that the variational approach is not contributing significantly to the accuracy of the calculated reaction barriers in these reactions.

Comparing next the barriers at the G3(MP2)-RAD and RMP2/6-311+G(3df,2p) levels of theory, we note that at the formal transition structures the forward barriers for reactions 1−4 differ by less than 2 kJ mol^{-1}; however, those for reactions 5 and 6 show substantially larger errors, 14.2 and 7.7 kJ mol^{-1}, respectively. Thus, as in the case of reaction enthalpies,[48] the RMP2/6-311+G(3df,2p) method performs well for the addition of the non-spin-contaminated radicals such as $\bullet CH_3$ (for which $\langle S^2\rangle = 0.76$ at the HF/6-31G(d) level of theory) or $\bullet CH_2COOCH_3$ ($\langle S^2\rangle = 0.79$) but shows larger errors for the addition of spin-contaminated radicals such as benzyl ($\langle S^2\rangle = 1.40$) and $\bullet C(CH_3)_2CN$ ($\langle S^2\rangle = 0.89$).[51] Interestingly, the errors in the reverse (i.e., fragmentation) barriers are considerably smaller, less than 5 kJ mol^{-1} for all of the reactions and less than 2 kJ

TABLE 3: Effect of Level of Theory on the Calculated Forward (s^{-1}) and Reverse (L mol^{-1} s^{-1}) Rate Coefficients for R• + S═C(Z)SCH_3 → R−SC•(Z)SCH_3 at 60 °C[a]

TS[b]	Z	R	VTST (HR)	VTST (HO)	TST (HO)	HR/HO	TST/VTST
			Forward Direction (Addition)				
1	CH_3	CH_3	1.18×10^6	6.81×10^5	1.08×10^7	1.7	15.8
2	phenyl	CH_3	5.47×10^7	2.99×10^7	1.99×10^8	1.8	6.7
3	benzyl	CH_3	8.79×10^6	1.87×10^6	2.42×10^7	4.7	12.9
4	CH_3	CH_2COOCH_3	1.19×10^8	4.03×10^7	6.27×10^7	2.9	1.6
5	CH_3	benzyl	2.76×10^6	4.67×10^5	4.67×10^5	5.9	1.0
6	CH_3	$C(CH_3)_2CN$	8.29×10^5	3.21×10^5	4.12×10^5	2.6	1.3
			Reverse Direction (Fragmentation)				
1	CH_3	CH_3	1.73	4.88	7.71×10^1	$(2.8)^{-1}$	15.8
2	phenyl	CH_3	3.67×10^{-4}	1.26×10^{-2}	8.37×10^{-2}	$(34.3)^{-1}$	6.7
3	benzyl	CH_3	8.63×10^{-2}	6.98×10^{-1}	9.01	$(8.1)^{-1}$	12.9
4	CH_3	CH_2COOCH_3	1.27×10^5	5.56×10^5	8.65×10^5	$(4.4)^{-1}$	1.0
5	CH_3	benzyl	7.15×10^5	6.06×10^6	6.06×10^6	$(8.5)^{-1}$	1.6
6	CH_3	$C(CH_3)_2CN$	6.21×10^7	1.89×10^8	2.42×10^8	$(3.0)^{-1}$	1.3

[a] All rate coefficients were calculated at the G3(MP2)-RAD//B3-LYP/6-31G(d) level of theory. The VTST (HR) value is the highest-level value and was evaluated at the variationally optimized transition structure and using a full hindered-rotor treatment of the low-frequency torsional modes. The VTST (HO) value differs from the VTST (HR) value only in the use of the harmonic oscillator approximation for all modes. The TST (HO) value also uses the harmonic oscillator approximation and was evaluated at the formal B3-LYP/6-31G(d) transition structure. [b] See Figure 1.

mol^{-1} for reactions 5 and 6. This further confirms that the error in these latter systems is largely associated with the leaving group radical, R•. In these spin-contaminated cases, it might thus be possible to obtain accurate results for the reaction R• + S═C(Z)SCH_3 via an ONIOM[52]-type approach in which the (exact) G3(MP2)-RAD barriers or enthalpies for the corresponding Z = CH_3 system are corrected for the Z-substituent effect, as calculated using the RMP2/6-311+G(3df,2p) level of theory.

When the G3(MP2)-RAD and RMP2/6-311+G(3df,2p) barriers are compared at the variational transition structures, the errors for the •CH_3 addition reactions are somewhat larger (6.1−9.4 kJ mol^{-1}) than at the formal transition structures (0.2−0.6 kJ mol^{-1}). It seems that the RMP2/6-311+G(3df,2p) method is overestimating the curvature of the potential energy surface for these reactions. While this suggests that the use of RMP2 energies in the search for the variational transition structures may be unwise, it should be noted that for the non-methyl radicals the errors at the variational transition structures were very similar to those at the formal transition structures. Hence, the problem may be restricted to the •CH_3 addition reactions and may not be significant in the larger polymer-related systems. Moreover, the large changes in the forming bond lengths between the B3-LYP/6-31G(d) (2.766−2.858 Å) and IRCmax (2.450−2.498 Å) transition structures for the •CH_3 addition reactions are similar to those reported previously (but at a much higher level of theory) for the related system •CH_3 + S═C$(CH_3)_2$.[53] Thus, as a tool for optimizing the transition state geometries via IRCmax, the RMP2/6-311+G(3df,2p) method appears to be yielding realistic results.

On the basis of the barrier heights, one might conclude that, provided the transition structures are optimized at a high enough level of theory (using, for example, an IRCmax technique), the use of variational transition-state theory does not appear to be contributing significantly to the accuracy of the results and might thus be neglected in favor of standard transition-state theory. However, when the reaction rates are examined, it is clear that the variational approach is affecting the entropies of activation and hence the reaction rates. Table 3 shows the forward and reverse reaction rates for the six reactions, as calculated using the G3(MP2)-RAD barriers, but differing in their treatment of the low-frequency torsional modes and in the use of formal or variational transition-state theory. From Table 3, we see that the corresponding variational and standard transition-state theory rates differ by up to a factor of 15.8, of which the significant portion (up to a factor of 8.6) arises in the reaction entropy. Nonetheless, for the non-methyl addition reactions (which are more indicative of real polymer systems), the errors are negligible (less than a factor of 2), and it appears that formal transition-state theory may be adopted in place of variational transition-state theory without incurring significant additional error.

Comparing next the harmonic oscillator and hindered-rotor rate coefficients in Table 3, we note that the errors in the rate coefficients are smaller than those reported previously for the equilibrium constants of these reactions,[17] but not insignificant. In the addition reactions, the harmonic oscillator approximation leads to an underestimation of the rate coefficient, though the errors are lower than a factor of 10 and comparable to those reported previously for radical addition to alkenes.[36,41,54] In the fragmentation reactions, the harmonic oscillator model leads to an overestimation of the rate coefficients by up to a factor of 34.2, though the errors are generally lower than a factor of 10. Although it appears that the harmonic oscillator approximation may be suitable for qualitative order-of-magnitude calculations, it should be used cautiously for two reasons: First, because the errors in individual modes are multiplicative, one might expect the errors to be larger in some of the more complicated polymer-related systems. Second, the errors in the addition and fragmentation constants reinforce (rather than cancel) each other in the equilibrium constant of the reaction, leading to a significant underestimation of this parameter. Because the equilibrium constant plays an important role in the overall RAFT kinetics (determining, for example, the rate at which steady state is achieved[55]), it would thus be advisable to use the hindered-rotor model in quantitative studies of RAFT kinetics.

It is of interest to examine the main sources of error in the harmonic oscillator approximation for these reactions, as this understanding may assist in determining whether a hindered-rotor treatment is necessary for related reactions. To this end, a complete listing of the entropy and enthalpy associated with each low-frequency mode, as calculated under the hindered-rotor and harmonic oscillator models, is provided in Table S3 of the Supporting Information. One of the main sources of error arises in the treatment of the rotations about each of the S−C• single bonds in the product radical. The harmonic oscillator model underestimates the entropy associated with each of these modes by as much as 15 J mol^{-1} K^{-1}. These errors do not cancel

from the equilibrium constant of the reaction, because in the isolated reactants, one of these modes is entirely absent, and the other is part of the relatively rigid S—C═S system and is reasonably well-approximated by the harmonic oscillator model (the errors being on the order of 2 J mol^{-1} K^{-1}). In the transition structures, the S—C bonds are intermediate in character to those in the reactants and products, as is the error associated with their treatment under the harmonic oscillator model. As a result, in the addition reactions, there is a net underestimation of the entropy of activation (and hence the rate coefficient), but the error is smaller than in the equilibrium constant. In the fragmentation reactions, the error in the RAFT-adduct radical is larger than that in the transition structure and thus partially (but not totally) cancels from the entropy of activation. As a result, the rate coefficient is overestimated using the harmonic oscillator model, but the error is again much smaller than that in the equilibrium constant.

Errors in the other low-frequency torsional modes also contribute to the errors in the harmonic oscillator treatment of the rate coefficients and equilibrium constants for these reactions. For example, in reaction 2, the phenyl rotation is overestimated by 2.8 J mol^{-1} K^{-1} in the reactant and underestimated by 4.5 and 10.7 J mol^{-1} K^{-1} in the transition structure and product radicals, respectively. These errors reinforce those associated the S—C• rotations. In reaction 3, the corresponding errors in the phenyl rotation in the reactant, transition structure, and product radical are −3.6, 7.3, and 0.7 J mol^{-1} K^{-1}, respectively, while in reaction 5, they are 0, 9.5, and 1.2 J mol^{-1} K^{-1}, respectively. For these reactions, the errors reinforce those associated with S—C• rotations in the addition reactions but cancel some of the error in the fragmentation reactions. The benzyl rotations in reactions 3 and 5 are also poorly treated under the harmonic oscillator model. In the case of reaction 3, the errors in the reactant, transition structure, and product radical are, respectively, 5.8, 8.3, and 14.1 J mol^{-1} K^{-1}, and these reinforce those associated with the S—C• rotations. In reaction 5, the corresponding errors are 0, 9.5, and 8.3 J mol^{-1} K^{-1}, this time reinforcing the addition errors but not contributing significantly to the errors in the fragmentation constant. Finally, the fragmentation rate coefficient for reaction 2 is particularly badly treated under the harmonic oscillator model, because in addition to the other errors, the rotation about the forming bond is overestimated in the transition structure by 9.5 J mol^{-1} K^{-1}. While this error cancels some of the error in the addition rate coefficient, it serves to reinforce the error in the fragmentation rate coefficient.

To summarize, the addition—fragmentation kinetics in RAFT polymerization are a difficult theoretical problem and, where possible, high-level ab initio calculations, combined with variational transition-state theory and a hindered-rotor treatment of the low-frequency torsional modes should be adopted. However, when this is not practicable, it appears that reasonable results may be achievable using a simplified methodology. In particular, the present results indicate that standard transition-state theory may be adopted in favor of variational transition-state theory, and for non-spin-contaminated leaving group radicals, the RMP2/6-311+G(3df,2p) method may be used for the ab initio calculations. When spin-contaminated radicals, such as benzyl, are involved, an ONIOM-type procedure in which the effect of the leaving group is modeled at the high level of theory, but the effect of the Z-group is modeled at the RMP2/6-311+G(3df,2p) level, should provide reasonable results. It also appears that the harmonic oscillator model may be used for qualitative order-of-magnitude studies of the kinetics of the individual reactions; however, for quantitative studies of RAFT kinetics, a hindered-rotor treatment of the low-frequency modes is advisable.

Addition—Fragmentation Kinetics. From the results in Table 1, it is seen that addition of carbon-centered radicals to C═S double bonds is a relatively fast reaction, typically around three orders of magnitude faster than addition to the C═C bonds of alkenes. For example, the rate coefficient for the addition of $\bullet CH_3$ to the simplest RAFT substrate $S{=}C(CH_3)SCH_3$ is 1.18×10^6 L mol^{-1} s^{-1} at 60 °C. The corresponding gas-phase rate coefficients for $\bullet CH_3$ addition to alkenes such as $CH_2{=}CH_2$, $CH_2{=}CHCH_3$, $CH_2{=}CHC_2H_5$, $CH_2{=}C(CH_3)_2$, $CH_2{=}CHF$, and $CH_2{=}CHCl$ are on the order of 10^3 L mol^{-1} s^{-1} at the same temperature.[56,57] As discussed previously,[58] the enhanced reactivity of the C═S double bond arises predominantly in its low singlet—triplet gap (typically lower than that of corresponding alkenes by over 2 eV), and this in turn is a reflection of weaker π-bonding interaction in the longer C═S bond. As a result of this low singlet—triplet gap, the addition reaction remains fast (compared with addition to alkenes), even when the exothermicity is low. Thus, for example, in reaction 5, although the exothermicity is only 30.7 kJ mol^{-1} at 60 °C, the addition rate coefficient remains high (2.7×10^6 L mol^{-1} s^{-1}). As a result, it is possible to design RAFT agents with relatively fast rate coefficients for *both* their forward and reverse reactions, a feature that is essential to the success of the process.

Additional features of the addition—fragmentation kinetics are the negative reaction barriers that are obtained for a number of the addition reactions. It was these negative barriers that inspired the use of variational transition-state theory in the present work, although (as seen already) it did not, in fact, contribute significantly to the accuracy of the results. The negative reaction barriers may simply be artifacts of the levels of theory used in their calculation. It should be noted that the B3-LYP/6-31G(d) optimized transition structures are true first-order saddle points with positive reaction barriers, which become negative when the energies are improved with higher-level RMP2/6-311+G(3df,2p) and G3(MP2)-RAD calculations. This in itself further illustrates poor accuracy of the B3-LYP method for studying the energetics of these radical addition reactions, a feature that has been highlighted previously.[26] Nonetheless, the curvature in the potential energy surface certainly remains at the higher RMP2/6-311+G(3df,2p) level of theory, despite the fact that the barriers become negative in some cases (see Figure S4 of the Supporting Information), and this would imply that at the RMP2/6-311+G(3df,2p) level the three reactions with negative barriers are preceded by weak complex formation. In the case of the $\bullet CH_2COOCH_3$ addition (4), there is certainly evidence that H-bonding interactions between the reactants may be occurring (see following text). Moreover, in the preferred conformations of the other two transition structures (5 and 6), the reactants are also orientated in such a manner that through-space interactions could be possible (see Figure 1). However, there was evidence in the comparison of the RMP2/6-311+G(3df,2p) and G3(MP2)-RAD levels of theory (discussed already) that the former may be overestimating the curvature of the potential energy surface for these reactions. Hence, it is also possible that these reactions are truly barrierless in the addition direction. In such a case, the free energy "barrier" to the reaction arises from the fact that the reactions are all strongly exothermic and exentropic (i.e., $-T\Delta S^{\ddagger}$ for the reaction is positive), and thus, the opposing enthalpic and entropic factors lead to a maximum in $\Delta G^{\ddagger}$ at some intermediate distance along the reaction path.[59]

As a result of the high reactivity of the C═S bond, and the early transition structures for the addition reactions, the effects of the substituents on the forward (i.e., addition) reactions are much smaller than those on the reverse (i.e., fragmentation) reactions. The addition rate coefficients vary by approximately 2 orders of magnitude over the 6 reactions, while the fragmentation rate coefficients vary by an enormous 11 orders of magnitude. In both directions, the qualitative effects of the substituents on the rate coefficients largely follow those on the equilibrium constants of the reactions (which can be calculated from Table 1 as $K_{eq} = k_{add}/k_{frag}$), though there are some important exceptions. These trends in the equilibrium constants have been discussed elsewhere,[17] but to recap the principal features, the fragmentation reaction ($CH_3SC\bullet(Z)S-R \rightarrow CH_3SC(Z)=S + \bullet R$) is favored by R-substituents that are either bulky (and hence destabilize the breaking S−R bond of RAFT-adduct radical) and/or good radical-stabilizing substituents (which of course stabilize the product R• radical) but is disfavored by radical-stabilizing Z-substituents, as these stabilize the reactant RAFT-adduct radical. The effect of the Z-substituent on the stability of the $CH_3SC(Z)=S$ product of fragmentation is also important, particularly when the Z-group is an electron donating substituent, such as an alkoxy or amine group.[20,60−68]

Applying these ideas to the fragmentation constants in Table 1, we note that the R = CH_3 reactions 1−3 have slower fragmentation rates than the other reactions, which reflects the smaller steric bulk and lower radical stability of the leaving $\bullet CH_3$ radicals. Within this series of reactions, the Z = phenyl system (2) has the slowest fragmentation rate, reflecting the strong resonance stabilization of the $CH_3SC\bullet(Ph)SCH_3$ radical. However, the Z = benzyl system has a smaller fragmentation rate than the Z = CH_3 system, despite the similar radical-stabilizing abilities of the Z-substituents. This trend, which was noted previously in the equilibrium constants, arises in the entropies (rather than enthalpies) of the reaction and probably reflects the greater relief of steric strain when the S═C(Bz)-SCH_3 RAFT agent is converted to the (more flexible) RAFT-adduct radical.

Considering next the reactions with the non-methyl leaving groups (4−6), we note that the R = $C(CH_3)_2CN$ reaction (6) has the fastest fragmentation rate, reflecting the combination of its large steric bulk and its relatively high stability as a leaving radical. The R = benzyl system (5) also has a fast fragmentation rate coefficient, but the reaction is slower than that for R = $C(CH_3)_2CN$. This is despite the fact that the benzyl radical (58.9 kJ mol^{-1})[69] has an almost identical radical stabilization energy to that of $\bullet C(CH_3)_2CN$ (59.0 kJ mol^{-1}).[17] Indeed, the fragmentation enthalpies for these two reactions are almost identical, and the faster fragmentation of the $\bullet C(CH_3)_2CN$ radical arises largely from entropic factors. Nonetheless, the barrier for R = Bz fragmentation is slightly higher than that for R = $C(CH_3)_2CN$, which indicates that polar stabilization of transition structure may be playing a role in the latter case. In support of this notion, it should be noted that there is a slight negative charge (−0.09 e) on the attacking $\bullet C(CH_3)_2CN$ radical in the transition structure and a negligible charge on the attacking benzyl radical (−0.01 e) in the corresponding R = benzyl reaction.[70] The present results thus support the earlier suggestion that polar effects are responsible for the larger transfer constants of RAFT agents bearing the $C(CH_3)_2CN$ group, compared with those bearing a cumyl group, despite the similar radical stabilities of the leaving groups.[60]

While the trends for the other reactions largely follow those in the equilibrium constants, the fragmentation kinetics for the R = CH_2COOCH_3 system (4) does not. The fragmentation rate for this reaction is much faster than it should be on the basis of its enthalpy and, indeed, its equilibrium constant (which, in the addition direction, is three orders of magnitude larger than the corresponding R = benzyl system[17]). This unusual result may be due to the stabilization of the transition structure by direct (possibly H-bonding) interactions between a hydrogen atom on the SCH_3 group of the RAFT agent and the carbonyl oxygen of the attacking radical. As can be seen in Figure 1, these lie within 2.5 Å of one another, close enough for hydrogen bonding to be playing a role. Similar types of interactions were postulated previously to account for unusual substituent effects in $\bullet CH_2OCOCH_3$ radical addition to xanthates of the form (S═C(OZ′)-SCH_3; Z′ = Me, Et, *i*-Pr, and *t*-Bu).[20]

In the addition direction, the substituent effects are much smaller; however, the trends loosely follow those in the equilibrium constants. For example, the bulky and stable $\bullet C(CH_3)_2CN$ attacking radical has the smallest rate coefficient, while the smaller and less stable $\bullet CH_3$ attacking radicals have much larger rate coefficients. Within the R = CH_3 series of reactions, the addition rate coefficient is smallest for the Z = phenyl system (2), reflecting the stability of the product radical in this case. However, as in the case of the fragmentation rate coefficients, the R = CH_2COOCH_3 system has an unusually high rate coefficient, reflecting some additional stabilization of the transition structure, probably involving direct (H-bonding) interactions between hydrogens on the RAFT agent and the carbonyl oxygen of the attacking radical. It is also worth noting that the addition of the benzyl radical to $S=C(CH_3)SCH_3$ (5) is slightly faster than that of the $\bullet CH_3$ radical (1), a difference that arises from a lower reaction barrier in the former case. This trend is somewhat unusual, the benzyl radical being both larger and more stable than $\bullet CH_3$. Moreover, given the negligible charge separation in its transition structure, the faster rate coefficient for benzyl addition does not appear to be related to favorable polar interactions. It is possible that some form of direct interaction between the reactants are occurring, though it is difficult to identify the exact nature of these interactions at the present time. In any case, it should be stressed that the effects are relatively small, and possibly within the level of error in the calculated rate coefficients.

Finally, it is worth commenting on the relationship between the current calculated rate coefficients and the experimental values for RAFT polymerization systems. In the present work, rate coefficients have been calculated for prototypical systems to allow for a detailed, accurate study of both the methodology and the individual effects of the R- and Z-substituents. To make direct comparisons with real polymerization systems, such as styrene polymerization at 60 °C with cumyl dithiobenzoate, it would be necessary to consider the effects of the R- and Z-substituents simultaneously (for example, a prototypical reaction such as $\bullet CH_2Ph + S=C(Ph)SCH_3$ might be studied). Furthermore, given the sensitivity of the addition and fragmentation reactions to steric factors, the effect of the chain length would also need to be considered in comparisons with polymeric systems. Despite these limitations, it is gratifying to note that the calculated addition rate coefficients fall into the range of generally accepted values for polymeric systems, such as styrene at 60 °C with cumyl dithiobenzoate (CDB) ($k_{add} = 5.4 \times 10^5$ or 4×10^6 L mol^{-1} s^{-1})[10,13,19] or cumyl phenyldithioacetate ($k_{add} = 5.4 \times 10^5$ L mol^{-1} s^{-1}).[71] In this regard, it makes sense to compare these polymeric values with the most sterically hindered k_{add} value in Table 1, that for the R = $C(CH_3)_2CN$ system ($k_{add} = 8.3 \times 10^5$ L mol^{-1} s^{-1}). Obviously, the electronic

effects of the R- and Z-substituents should be taken into account in making quantitative predictions of k_{add}; however, because these effects are relatively small, it can be concluded that the theoretical calculations are in reasonable qualitative agreement with the experimental polymeric values.

As outlined in the Introduction, the magnitude of the fragmentation rate coefficient in RAFT polymerization remains a major source of controversy in the polymer field, with alternative experimental values for the styrene/cumyl dithiobenzoate system differing by 6 orders of magnitude and implying different mechanistic descriptions of the RAFT process.[10−14] The a priori prediction of the rate coefficients for these reactions could help to discriminate between these alternative experimental estimates and hence provide information on the RAFT mechanism. Unfortunately, such discrimination cannot be carried out with the present data. As demonstrated in the present work, the fragmentation rate coefficient (in contrast to the addition rate coefficient) is extremely sensitive to the nature of the R- and Z-substituents (varying by 11 orders of magnitude over the small set of substituents considered in the present work). As a result, it is essential that the R- and Z-substituents in the model RAFT reactions capture the main chemical features of the RAFT polymerization system. Thus, for example, in the CDB/styrene system, the appropriate chemical model should, in the very least, simultaneously contain a phenyl Z-substituent and a benzyl leaving group (i.e., $CH_3SC\bullet(Ph)S-CH_2Ph \rightarrow CH_3SC(Ph)=S + \bullet CH_2Ph$). It has previously been shown that ab initio calculations of the equilibrium constants for this model system support those values associated with the slower values for the fragmentation rate coefficient.[17] More recently, this conclusion has been confirmed using the larger (and more realistic) cumyl leaving group.[18] Nonetheless, it would be desirable to calculate the fragmentation rate coefficients for realistic polymerization systems, and such calculations are currently underway.

Conclusions

In the present work, the forward and reverse rate coefficients have been calculated for a series of prototypical RAFT reactions: $R\bullet + S=C(Z)SCH_3 \rightarrow R-SC\bullet(Z)SCH_3$, for R = CH_3, with Z = CH_3, Ph, and CH_2Ph; and for Z = CH_3, with R = (CH_3), CH_2COOCH_3, CH_2Ph, and $C(CH_3)_2CN$. It was found that the addition of carbon-centered radicals to the sulfur center of C=S double bonds is a relatively fast reaction, typically around 3 orders of magnitude faster than addition to the C=C bonds of alkenes. As a result of the high reactivity of the C=S bond, and the early transition structures for the addition reactions, the effects of the substituents on the forward (i.e., addition) reactions are much smaller than those on the reverse (i.e., fragmentation) reactions. The addition rate coefficients vary by approximately 2 orders of magnitude over the 6 reactions, while the fragmentation rate coefficients vary by an enormous 11 orders of magnitude. In both directions, the qualitative effects of the substituents on the rate coefficients largely follow those on the equilibrium constants of the reactions. Thus, fragmentation is favored (and addition is disfavored) by bulky and radical-stabilizing R-groups, and addition is favored (and fragmentation disfavored) by bulky and radical-stabilizing Z-groups. However, there are some important additional factors influencing the kinetics of the reactions. In particular, the addition and fragmentation rates for the R = CH_2COOCH_3 system are both significantly higher than they should be on the basis of the equilibrium constant, and this appears to be the result of the stabilizing influence of direct (H-bonding) interactions in the transition structure. There is also evidence that charge-transfer stabilization of the transition structure is contributing a barrier-lowering influence to the R = $C(CH_3)_2CN$ system.

As part of this work, various methodological issues in the calculation of rate coefficients for model RAFT polymerization systems were examined. In general, it was found that the addition−fragmentation kinetics in RAFT polymerization are a difficult theoretical problem, and where possible, high-level ab initio calculations (such as G3(MP2)-RAD) combined with variational transition-state theory and a hindered-rotor treatment of the low-frequency torsional modes should be adopted. However, when this is not practicable, it appears that reasonable results may be achievable using standard transition-state theory. Moreover, for the non-spin-contaminated leaving group radicals, the considerably cheaper RMP2/6-311+G(3df,2p) method may be used for the ab initio calculations. When delocalized radicals, such as benzyl, are involved, reasonable results might be obtained using an approximate G3(MP2)-RAD procedure, based on an ONIOM-type approach. It also appears that the harmonic oscillator model may be used for qualitative order-of-magnitude studies of the kinetics of the individual reactions; however, for quantitative studies of RAFT kinetics, a hindered-rotor treatment of the low-frequency modes is advisable.

Acknowledgment. Generous allocations of computing time on the Compaq Alphaserver and the Linux Cluster of the Australian Partnership for Advanced Computing and the Australian National University Supercomputer Facility, useful discussions with Professor Leo Radom, and provision of an Australian Research Council postdoctoral fellowship are all gratefully acknowledged.

Supporting Information Available: Table S1 shows the B3-LYP/6-31G(d) optimized geometries (in the form of Gaussian archive entries) for species **1**−**6** in Figure 1, both as variational and formal transition structures. Tables S2 and S3 show the rotational potentials (or barriers) corresponding to thermodynamic functions for the modes treated as hindered internal rotations. These modes are defined in Figures S1−S3. Table 4 shows the variation in enthalpy, entropy, and Gibb's free energy along the reaction path for each reaction; these data are also plotted in Figure S4. This material is available free of charge via the Internet at http://pubs.acs.org.

References and Notes

(1) Hawker, C. J.; Bosman, A. W.; Harth, E. *Chem. Rev.* **2001**, *101*, 3661−88.

(2) Wang, J. S.; Matyjaszewski, K. *J. Am. Chem. Soc.* **1995**, *117*, 5614−5615.

(3) Chiefari, J.; Chong, Y. K. B.; Ercole, F.; Krstina, J.; Jeffery, J.; Le, T. P. T.; Mayadunne, R. T. A.; Meijs, G. F.; Moad, C. L.; Moad, G.; Rizzardo, E.; Thang, S. H. *Macromolecules* **1998**, *31*, 5559−5562.

(4) Barner-Kowollik, C.; Dalton, H.; Davis, T. P.; Stenzel, M. H. *Angew. Chem., Int. Ed.* **2003**, *42*, 3664−3668.

(5) Kowalewski, T.; Tsarevsky, N. V.; Matyjaszewski, K. *J. Am. Chem. Soc.* **2003**, *124*, 10632−10633.

(6) Chen, M.; Ghiggino, K. P.; Launikonis, A.; Mau, A. W. H.; Rizzardo, E.; Saase, W. H. F.; Thang, S. H.; Wilson, G. J. *J. Mater. Chem.* **2003**, *13*, 2696−2700.

(7) Sumerlin, B. S.; Lowe, A. B.; Thomas, D. B.; McCormick, C. L. *Macromolecules* **2003**, *36*, 5982−5987.

(8) Lowe, A. B.; McCormick, C. L. *Aust. J. Chem.* **2002**, *55*, 367−379.

(9) Delduc, P.; Tailhan, C.; Zard, S. Z. *J. Chem. Soc., Chem. Commun.* **1988**, 308.

(10) Barner-Kowollik, C.; Quinn, J. F.; Morsley, D. R.; Davis, T. P. *J. Polym. Sci., Part A: Polym. Chem.* **2001**, *39*, 1353−1365.

(11) Barner-Kowollik, C.; Coote, M. L.; Davis, T. P.; Radom, L.; Vana, P. *J. Polym. Sci., Part A: Polym. Chem.* **2003**, *41*, 2828−2832.

(12) Wang, A. R.; Zhu, S.; Kwak, Y.; Goto, A.; Fukuda, T.; Monteiro, M. S. *J. Polym. Sci., Part A: Polym. Chem.* **2003**, *41*, 2833−2839.

(13) Kwak, Y.; Goto, A.; Tsuji, Y.; Murata, Y.; Komatsu, K.; Fukuda, T. *Macromolecules* **2002**, *35*, 3026−3029.
(14) Monteiro, M. J.; de Brouwer, H. *Macromolecules* **2001**, *34*, 349−352.
(15) Coote, M. L. *Aust. J. Chem.* **2004**, *57*, 1125−1132.
(16) Coote, M. L.; Radom, L. *J. Am. Chem. Soc.* **2003**, *125*, 1490−1491.
(17) Coote, M. L. *Macromolecules* **2004**, *37*, 5023−5031.
(18) Feldermann, A.; Coote, M. L.; Stenzel, M. H.; Davis, T. P.; Barner-Kowollik, C. *J. Am. Chem. Soc.* **2004**, *126*, 15915−15923.
(19) Goto, A.; Sato, K.; Tsujii, Y.; Fukuda, T.; Moad, G.; Rizzardo, E.; Thang, S. H. *Macromolecules* **2001**, *34*, 402.
(20) Coote, M. L.; Radom, L. *Macromolecules* **2004**, *37*, 590−596.
(21) Hehre, W. J.; Radom, L.; Schleyer, P. v. R.; Pople, J. A. *Ab Initio Molecular Orbital Theory*; Wiley: New York, 1986.
(22) Koch, W.; Holthausen, M. C. *A Chemist's Guide to Density Functional Theory*; Wiley-VCH: Weinheim, 2000.
(23) Frisch, M. J.; Trucks, G. W.; Schlegel, H. B.; Scuseria, G. E.; Robb, M. A.; Cheeseman, J. R.; Zakrzewski, V. G.; Montgomery, J. A., Jr.; Stratmann, R. E.; Burant, J. C.; Dapprich, S.; Millam, J. M.; Daniels, A. D.; Kudin, K. N.; Strain, M. C.; Farkas, O.; Tomasi, J.; Barone, V.; Cossi, M.; Cammi, R.; Mennucci, B.; Pomelli, C.; Adamo, C.; Clifford, S.; Ochterski, J.; Petersson, G. A.; Ayala, P. Y.; Cui, Q.; Morokuma, K.; Malick, D. K.; Rabuck, A. D.; Raghavachari, K.; Foresman, J. B.; Cioslowski, J.; Ortiz, J. V.; Stefanov, B. B.; Liu, G.; Liashenko, A.; Piskorz, P.; Komaromi, I.; Gomperts, R.; Martin, R. L.; Fox, D. J.; Keith, T.; Al-Laham, M. A.; Peng, C. Y.; Nanayakkara, A.; Gonzalez, C.; Challacombe, M.; Gill, P. M. W.; Johnson, B. G.; Chen, W.; Wong, M. W.; Andres, J. L.; Head-Gordon, M.; Replogle, E. S.; Pople, J. A. *Gaussian 98*; Gaussian, Inc.: Pittsburgh, PA, 1998.
(24) Werner, H.-J.; Knowles, P. J.; Amos, R. D.; Bernhardsson, A.; Berning, A.; Celani, P.; Cooper, D. L.; Deegan, M. J. O.; Dobbyn, A. J.; Eckert, F.; Hampel, C.; Hetzer, G.; Korona, T.; Lindh, R.; Lloyd, A. W.; McNicholas, S. J.; Manby, F. R.; Meyer, W.; Mura, M. E.; Nicklass, A.; Palmieri, P.; Pitzer, R.; Rauhut, G.; Schütz, M.; Stoll, H.; Stone, A. J.; Tarroni, R.; Thorsteinsson, T. *MOLPRO 2000.6*; University of Birmingham: Birmingham, Alabama, 1999.
(25) Henry, D. J.; Sullivan, M. B.; Radom, L. *J. Chem. Phys.* **2003**, *118*, 4849−4860.
(26) Coote, M. L.; Wood, G. P. F.; Radom, L. *J. Phys. Chem. A* **2002**, *106*, 12124−12138.
(27) Schwartz, M.; Marshall, P.; Berry, R. J.; Ehlers, C. J.; Petersson, G. A. *J. Phys. Chem. A* **1998**, *102*, 10074.
(28) See, for example, (a) Garrett, B. C.; Truhlar, D. G. *J. Chem. Phys.* **1979**, *70*, 1593−1598. (b) Truhlar, D. G.; Garrett, B. C. *Acc. Chem. Res.* **1980**, *13*, 440−448. (c) Stull, D. R.; Westrum, E. F., Jr.; Sinke, G. C. *The Thermodynamics of Organic Compounds*; John Wiley & Sons: New York, 1969. (d) Robinson, P. J. *J. Chem. Educ.* **1978**, *55*, 509−510. (e) Steinfeld, J. I.; Francisco, J. S.; Hase, W. L. *Chemical Kinetics and Dynamics*; Prentice Hall: Englewood Cliffs, New Jersey, 1989.
(29) These formulas are also summarized in the following: Coote, M. L. Computational Quantum Chemistry for Free-Radical Polymerization. In *Encyclopedia of Polymer Science and Technology*, 3rd ed.; Kroschwitz, J. I., Ed.; John Wiley and Sons: New York, 2004; Vol. 9, pp 319−371.
(30) Bell, R. P. *The Tunnel Effect in Chemistry*; Chapman and Hall: London , 1980.
(31) Truhlar, D. G.; Isaacson, A. D.; Skodje, R. T.; Garrett, B. C. *J. Phys. Chem.* **1982**, *86*, 2252.
(32) Truhlar, D. G.; Garrett, B. C. *J. Am. Chem. Soc.* **1989**, *111*, 1232.
(33) See, for example, Truhlar, D. G.; Garrett, B. C.; Klippenstein, S. J. *J. Phys. Chem.* **1996**, *100*, 12771−12800.
(34) Eckart, C. *Phys. Rev.* **1930**, *35*, 1303.
(35) Coote, M. L.; Collins, M. A.; Radom, L. *Mol. Phys.* **2003**, *101*, 1329−1338.
(36) Van Speybroeck, V.; Van Neck, D.; Waroquier, M.; Wauters, S.; Saeys, M.; Martin, G. B. *J. Phys. Chem. A* **2000**, *104*, 10939−10950.
(37) Pitzer, K. S.; Gwinn, W. D. *J. Chem. Phys.* **1942**, *10*, 428−440.
(38) Li, J. C. M.; Pitzer, K. S. *J. Phys. Chem.* **1956**, *60*, 466−474.
(39) East, A. L. L.; Radom, L. *J. Chem. Phys.* **1997**, *106*, 6655.
(40) (a) Nordholm, S.; Bacskay, G. B. *Chem. Phys. Lett.* **1976**, *42*, 253−258. (b) Bacskay, G. B. Unpublished computer program, written in Fortran.
(41) Heuts, J. P. A.; Gilbert, R. G.; Radom, L. *J. Phys. Chem.* **1996**, *100*, 18997−19006.
(42) Heuts, J. P. A.; Gilbert, R. G.; Radom, L. *Macromolecules* **1995**, *28*, 8771−8781.
(43) Van Speybroeck, V.; Van Neck, D.; Waroquier, M. *J. Phys. Chem. A* **2002**, *106*, 8945−8950.
(44) Gonzalez, C.; Schlegel, H. B. *J. Chem. Phys.* **1989**, *90*, 2154.
(45) Gonzalez, C.; Schlegel, H. B. *J. Phys. Chem.* **1990**, *94*, 5523.
(46) Baboul, A. G.; Schlegel, H. B. *J. Chem. Phys.* **1997**, *107*, 9413.
(47) Lynch, B. J.; Fast, P. L.; Harris, M.; Truhlar, D. G. *J. Phys. Chem. A* **2000**, *104*, 4811−4815.
(48) Coote, M. L.; Henry, D. J. *Macromolecules* **2005**, in press.
(49) Malick, D. K.; Petersson, G. A.; Montgomery, J. A. *J. Chem. Phys.* **1998**, *108*, 5704.
(50) Chuang, Y. Y.; Corchado, J. C.; Truhlar, D. G. *J. Phys. Chem. A* **1999**, *103*, 1140−1149.
(51) It should be noted that this spin contamination is, of course, absent in the corresponding ROMP2/6-311+G(3df,2p) calculations. However, the presence of spin contamination at the UHF level is likely to be a symptom of the increased multireference character of the true wavefunction in these delocalized radicals, and the use of a (single-reference) RO-wavefunction in these cases may be enforcing a greater degree of spin localization than would be present in the true wavefunction.
(52) Vreven, T.; Morokuma, K. *Theor. Chem. Acc.* **2003**, *109*, 125−132.
(53) In this previous work, it was found that the forming bond length at the B3-LYP/6-31G(d) level of theory (2.863 Å) was significantly overestimated compared with the higher QCISD/6-31G(d) level (2.579 Å). However, when corrected using the IRCmax technique at the CCSD(T)/6-311+G(d,p)//B3-LYP/6-31G(d) level, a forming bond length of 2.55 Å was obtained.
(54) Gómez-Balderas, R.; Coote, M. L.; Henry, D. J.; Radom, L. *J. Phys. Chem. A* **2004**, *108*, 2874−2883.
(55) Vana, P.; Davis, T. P.; Barner-Kowollik, C. *Macromol. Theory Simul.* **2002**, *11*, 823.
(56) Fischer, H.; Radom, L. *Angew. Chem., Int. Ed.* **2001**, *40*, 1340−1371.
(57) Using the standardized gas-phase Arrhenius parameters in Table 3 of ref 56, the calculated rate coefficients at 60 °C for $\bullet CH_3$ addition are 3.5×10^3 L mol^{-1} s^{-1} (for $CH_2{=}CH_2$), 2.0×10^3 L mol^{-1} s^{-1} (for $CH_2{=}CHCH_3$), 2.1×10^3 L mol^{-1} s^{-1} (for $CH_2{=}CHC_2H_5$), 5.2×10^3 L mol^{-1} s^{-1} (for $CH_2{=}C(CH_3)_2$), 2.3×10^3 L mol^{-1} s^{-1} (for $CH_2{=}CHF$), and 4.2×10^3 L mol^{-1} s^{-1} (for $CH_2{=}CHCl$).
(58) Henry, D. J.; Coote, M. L.; Gómez-Balderas, R.; Radom, L. *J. Am. Chem. Soc.* **2004**, *126*, 1732−1740.
(59) Sachchida, N. R.; Truhlar, D. G. *J. Chem. Phys.* **1983**, *79*, 6046−6059.
(60) Moad, G.; Chiefari, J.; Chong, Y. K.; Krstina, J.; Mayadunne, R. T. A.; Postma, A.; Rizzardo, E.; Thang, S. H. *Polym. Int.* **2000**, *49*, 993.
(61) Rizzardo, E.; Chiefari, J.; Mayadunne, R. T. A.; Moad, G.; Thang, S. H. *ACS Symp. Ser.* **2000**, *786*, 278−296.
(62) Stenzel, M. H.; Cummins, L.; Roberts, G. E.; Davis, T. P.; Vana, P.; Barner-Kowollik, C. *Macromol. Chem. Phys.* **2003**, *204*, 1160−1168.
(63) Destarac, M.; Charmot, D.; Franck, X.; Zard, S. Z. *Macromol. Rapid Commun.* **2000**, *21*, 1035.
(64) Mayadunne, R. T. A.; Rizzardo, E.; Chiefari, J.; Chong, Y. K.; Moad, G.; Thang, S. H. *Macromolecules* **1999**, *32*, 6977.
(65) Destarac, M.; Taton, D.; Zard, S. Z.; Saleh, T.; Six, I. *ACS Symp. Ser.* **2003**, *854*, 536−550.
(66) Destarac, M.; Bzducha, W.; Taton, D.; Gauthier-Gillaizeau, I.; Zard, S. Z. *Macromol. Rapid Commun.* **2002**, *23*, 1049−1054.
(67) Chiefari, J.; Mayadunne, R. T. A.; Moad, C. L.; Moad, G.; Rizzardo, E.; Postma, A.; Skidmore, M. A.; Thang, S. H. *Macromolecules* **2003**, *36*, 2273−2283.
(68) Adamy, M.; van Herk, A. M.; Destarac, M.; Monteiro, M. J. *Macromolecules* **2003**, *36*, 2293−2301.
(69) Henry, D. J.; Parkinson, C. J.; Mayer, P. M.; Radom, L. *J. Phys. Chem. A* **2001**, *105*, 6750−6756.
(70) NBO charges calculated at the B3-LYP/6-311+G(3df,2p)//B3-LYP/6-31G(d) level of theory.
(71) Barner-Kowollik, C.; Quinn, J. F.; Uyen Nguyen, T. L.; Heuts, J. P. A.; Davis, T. P. *Macromolecules* **2001**, *34*, 7849−7857.